PNAS RESEARCH ARTICLE | NEUROSCIENCE

A hierarchical cascade of sleep rhythms supports motor memory and is hijacked by epileptic spikes in human epilepsy

Anirudh Wodeyar[a,1], Dhinakaran Chinappen[b,c], Hunki Kwon[b,c], Wen Shi[d,e], R. Mark Richardson[e,f], Mark A. Kramer[g,h,2], and Catherine J. Chu[b,c,1,2]

Affiliations are included on p. 11.

Edited by James L. McGaugh, University of California, Irvine, CA; received July 17, 2025; accepted May 21, 2026

The cross-regional interplay of slow oscillations, spindles, and ripples during sleep is believed to support systems memory consolidation but remains understudied in humans. Using a validated behavioral task and simultaneous intracranial neural recordings from the orbitofrontal cortex, thalamus, and hippocampus in 19 patients with epilepsy, we examined the cross-regional interplay of sleep oscillations (slow oscillations, spindles, and ripples), alongside epileptic spikes, and their role in motor memory consolidation. Orbitofrontal slow oscillations robustly modulate spindle and ripple oscillations within and across regions during sleep. Although most combinations of oscillation rates positively predicted overnight performance change in a motor task, hippocampal ripple rate and coupled hippocampal-orbitofrontal ripple rates were the most reliable predictors across subjects. In contrast, rates of most sleep oscillations coupled to epileptic spikes were negative predictors of overnight motor performance change, with the rate of slow oscillations co-occurring with epileptic spikes the most reliable predictors of negative change across subjects. These findings provide direct evidence of a hierarchical cascade of sleep oscillations in human motor memory processing and reveal that epileptic spikes coupled to sleep oscillations interfere with this process in patients with epilepsy.

sleep | memory | epilepsy | electroencephalography | oscillations

Significance

Sleep-dependent memory consolidation is thought to rely on coordinated interactions among slow oscillations, spindles, and ripples across the cortex, thalamus, and hippocampus, but direct human evidence has been limited. Using simultaneous intracranial recordings from the orbitofrontal cortex, thalamus, and hippocampus in patients with epilepsy, we show that orbitofrontal slow oscillations organize spindle and ripple activity within and across regions during sleep. Hippocampal ripple activity, particularly when coupled with orbitofrontal ripples, was the most reliable positive predictor of overnight motor memory improvement. In contrast, epileptic spikes coupled to sleep oscillations, especially slow oscillations, predicted worse overnight performance. These findings provide direct human evidence for a hierarchical cross-regional sleep-oscillation process supporting motor memory consolidation and show how epilepsy disrupts that process.

Sleep is a critical period for the integration and strengthening of memories. Three cardinal sleep electrophysiological rhythms—slow oscillations (0.5 to 2 Hz), spindles (8 to 15 Hz), and ripples (70 to 120 Hz)—have been linked to non–rapid eye movement (non-REM) sleep-dependent memory consolidation (1–4). Available evidence suggests that slow oscillations originate primarily in the frontal cortex (5) before propagating across widespread regions (5, 6). Regional and generalized thalamocortical sleep spindles are initiated in the thalamus, coordinated with the up-state of slow oscillations (7–9). Ripples, a short (<100 ms) and temporally discrete oscillation in the hippocampus have been linked to offline memory replay (10, 11), and ripple-like focal events have now been detected throughout the human cortex (12–14). The interplay of slow oscillations, spindles, and ripples across the frontal cortex, thalamus, and hippocampus is thought to be crucial for systems memory consolidation (15, 16), though the precise coordination of these electrophysiological events across this anatomical circuit remains poorly understood.

Previous human studies have demonstrated pairwise coupling and temporal coordination among slow oscillations, spindles, and ripples in frontal regions, hippocampus, and thalamus (1, 8, 12, 17–21) replicating and extending analyses from rodent models (2, 3, 22–24). These studies have also shown that individual or pairwise combinations of sleep oscillations across different subsets of the neocortex, hippocampus, and thalamus predict memory consolidation (2–4, 11, 23, 25). However, despite these important insights into sleep oscillatory coordination and memory, the optimal integration of cardinal sleep rhythms across the broader circuit connecting the frontal cortex, thalamus, and hippocampus to support human memory remains unknown.

In parallel, memory concerns are the primary cognitive symptom reported in epilepsy, a disease characterized by pathologic neuronal synchronization (26–28). Memory symptoms in patients with epilepsy are frequent even in the absence of antiseizure medications, structural lesions, or frequent seizures. In wakefulness, epileptic spikes interfere with memory encoding (29–33). In sleep, epileptic spikes are facilitated by slow oscillations and "hijack" or disrupt spindles and ripples (9, 26, 34–36), however the impact that this disruptive interference of sleep oscillations has on sleep-dependent memory consolidation remains poorly understood.

To address these knowledge gaps, we evaluated sleep oscillations, epileptic spikes, and sleep-dependent motor memory consolidation in a cohort of patients with drug

The authors declare no competing interest.

This article is a PNAS Direct Submission.

[1]To whom correspondence may be addressed. Email: ani.wodeyar@maastrichtuniversity.nl or cjchu@jhu.edu.

[2]M.A.K. and C.J.C. contributed equally to this work.

This article contains supporting information online at https://www.pnas.org/lookup/suppl/doi:10.1073/pnas.2517454123/-/DCSupplemental.

Published June 30, 2026.

refractory epilepsy and intracranial electrophysiological recordings simultaneously sampling the medial orbitofrontal cortex, thalamus, and hippocampus. We examined the spatiotemporal coordination of slow oscillations, spindles, and ripples within and across the orbitofrontal cortex, thalamus, and hippocampus. We then evaluated the relationship of each oscillation and their combinations within and across brain regions to overnight performance change on a motor sequence typing task (MST). Next, we evaluated the impact of epileptic spikes alone and co-occurring with sleep oscillations on overnight MST performance change. Finally, we identified the optimal predictive model of overnight MST performance change from all combinations of events across all brain regions. Through this work, we provide evidence of a hierarchical cascade of network activity strongly modulated by frontal slow oscillations. We show that downstream ripple oscillations most reliably predict motor memory consolidation, while epileptic spikes coupled to slow oscillations at the top of this cascade most reliably interfere with this process. Our findings thus add significant detail to the general framework of systems memory consolidation.

Results

Subject Characteristics. All subjects admitted to the MGH Epilepsy Monitoring Unit with stereo-electroencephalography (SEEG) electrodes sampling medial orbitofrontal cortex (OFC), thalamus, and hippocampus between 5/2021 and 11/2023 were included. Nineteen subjects (26 sampled hemispheres) met these inclusion criteria. Fourteen subjects completed the motor sequence typing (MST) task (37–39) before and after sleep on the night analyzed. The MST is a widely used behavioral assay to probe offline motor memory consolidation where performance changes have been linked to the rates of slow oscillations, spindles, and hippocampal ripples (35, 40–42). Subject characteristics are provided in *SI Appendix*, Table S2.

Characteristic Slow Oscillations, Spindles, and Ripples Are Observed in Each Region. Slow oscillations, sleep spindles, and ripples were detected in all channels in all three regions during all bouts of stages 2 (N2) and 3 (N3) non–rapid eye movement sleep over a 12-h period using previously validated detectors (*Methods* and Fig. 1). For these analyses, sleep oscillations that co-occurred with epileptic spikes (see *Methods* for detection criteria) in any region were excluded. We found an average rate of 5.22/min (±0.21/min SE) for slow oscillations, 5.78 (±0.46)/min for spindles, and 3.19 (±0.21)/min for ripples. Slow oscillation and spindle rates were higher in the OFC and thalamus than in the hippocampus (comparison-corrected $P < 0.05$), while ripple rates were highest in the hippocampus (comparison-corrected $P < 0.05$). For details on rates within each region and the statistical testing, please see *SI Appendix*, Table S1.

Slow Oscillation Downstate Troughs Occur First in the OFC and Coordinate Across the Thalamus and Hippocampus. Visual inspection of the average voltage trace across subjects demonstrates that slow oscillations are strongly temporally coordinated across regions (Fig. 2*A*). A triphasic slow oscillation appeared in each region, with an initial up-state peak near −0.5 s and a second up-state peak near +0.5 s relative to the downstate trough. On average, the slow oscillation downstate trough occurred first in the medial OFC, followed by the thalamus [15.6 ± 2.7 ms later, T(25) = 5.877, P = 3.9e-6], and then the hippocampus [35.1 ± 12.3 ms later, T(25) = 2.86, P = 0.0085]. We found qualitatively consistent temporal ordering but greater variability in the estimated delays (thalamus: 11.7 ± 17.3 ms later; hippocampus: 32.9 ± 29.8 ms later) when referencing events relative to the positive-to-negative zero-crossing prior to the downstate trough, consistent with the

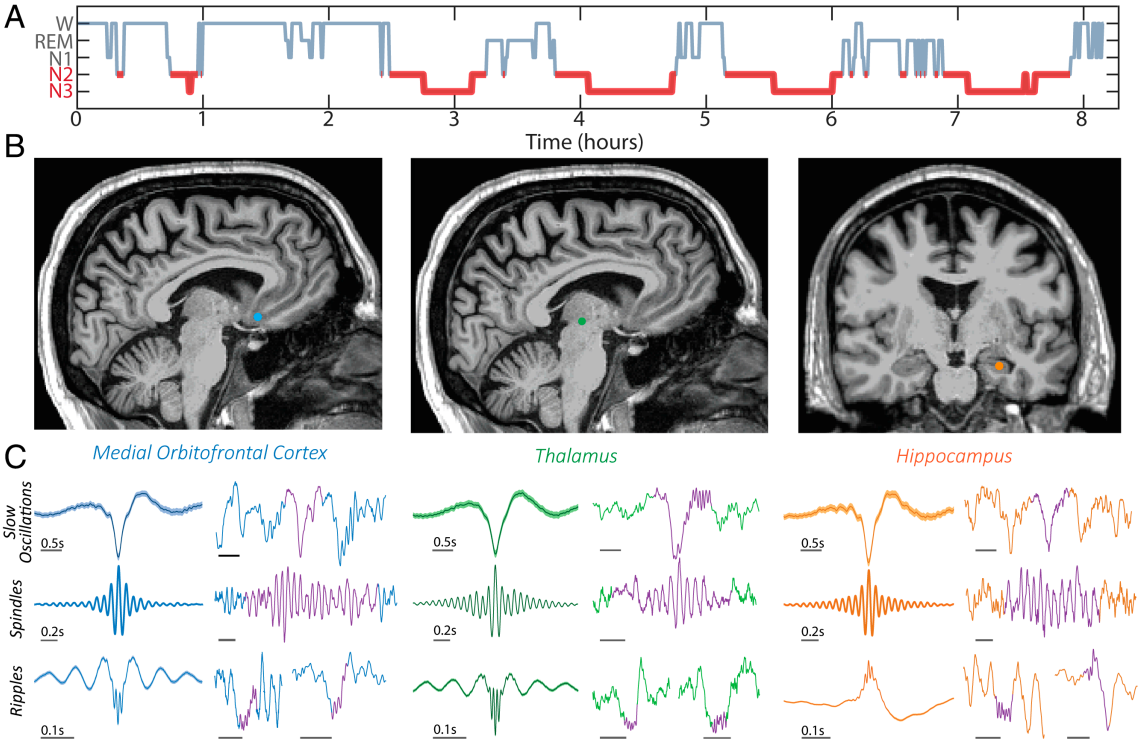

Fig. 1. Canonical rhythms of sleep are observed in the human cortex, thalamus, and hippocampus. (*A*) Example overnight hypnogram from one subject where N2 and N3 epochs were selected for analysis (red). (*B*) Example SEEG lead locations in one subject sampling OFC (blue circle), thalamus (green circle), and hippocampus (orange circle). (*C*) Example averaged (*Left*) and individual (*Right*, purple) slow oscillations, spindles, and ripples detected in each location. All oscillatory events detected for one subject are used to generate the average waveforms. Amplitudes rescaled for visualization.

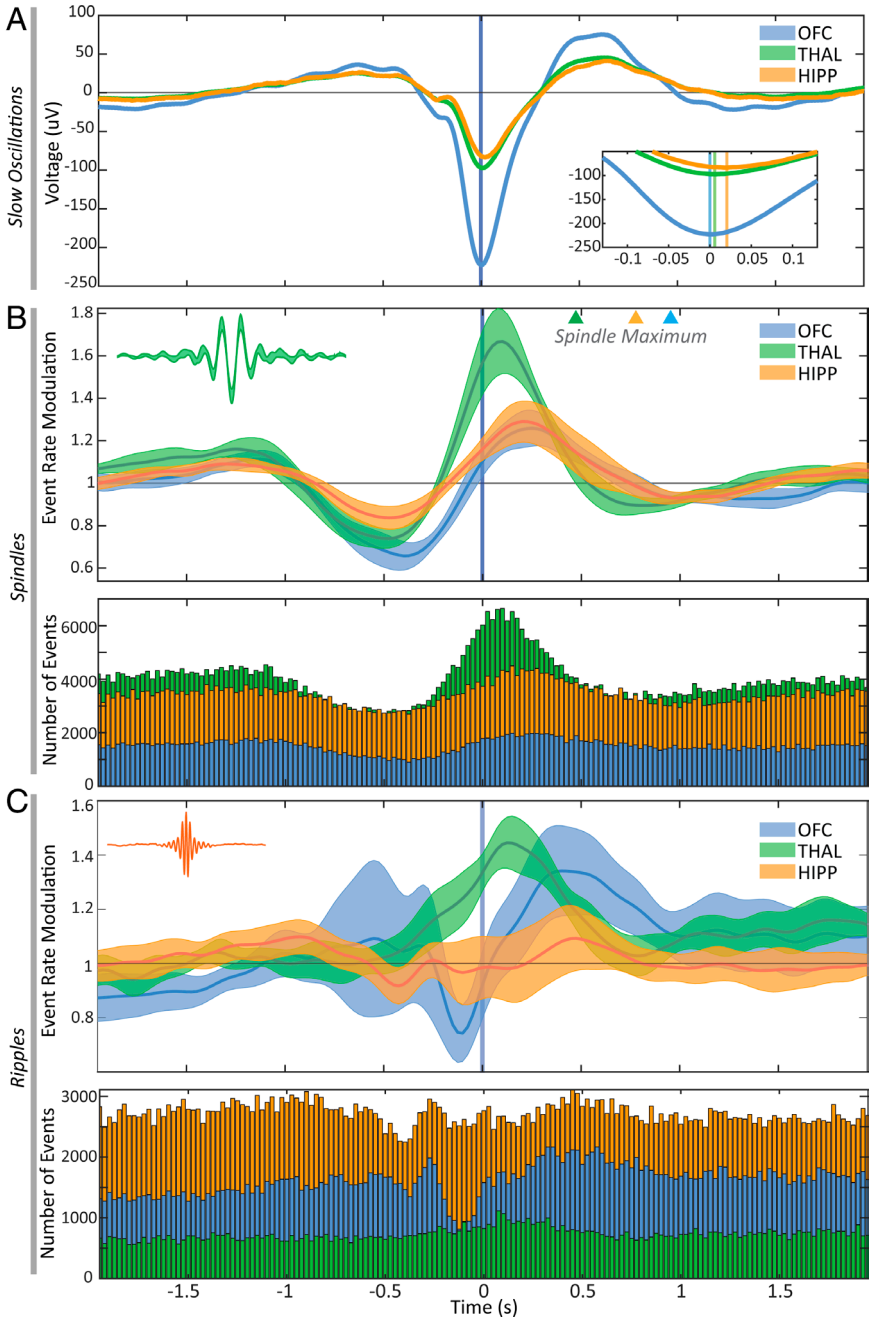

Fig. 2. Cross-regional coupling of slow oscillations, spindles, and ripples in humans during sleep. (*A*) All detected slow oscillations temporally aligned to the medial orbitofrontal cortex (OFC, blue) slow oscillation downstate trough. (*Inset*) The minima of averaged events are observed first in the OFC followed by the thalamus (green) then hippocampus (orange). (*B*) (*Upper*) Modulation in incidence relative to baseline spindle rates in the OFC, thalamus, and hippocampus temporally aligned to the OFC slow oscillation minima. Triangles show the spindle amplitude maxima, which coincide with the slow oscillation up-state. (*Lower*) Total number of spindles detected in each region (25 ms time bins). (*C*) (*Upper*) Modulation in incidence of ripples in the OFC, thalamus, and hippocampus temporally aligned to the OFC slow oscillation trough. (*Lower*) Total number of ripples detected in each region (25 ms time bins). Shaded areas indicate corrected 95% CI.

trough providing a more stable temporal reference. We note that volume conduction could produce the same slow oscillation in the cortex, thalamus, and hippocampus; however, volume conduction is approximately instantaneous (43), whereas we detect a delay across regions. Alternatively, signals in each region could be a superposition of a shared far-field slow oscillation and temporally consistent local activity (e.g., local slow oscillations or spindle activity), yielding regionally specific slow oscillation morphologies that produce the observed delay structure. However, we would not expect superimposed random activity to generate the consistent observations reported here across subjects and brain structures. The presence of an OFC slow oscillation predicted an up-regulation of thalamic slow oscillation occurrences by a factor of 9.33 (95% adjusted CI [8.1, 10.25], corrected $P < 0.05$, see *Statistical Analysis* for details), and hippocampal slow oscillation occurrences by a factor of 5.37 (95% CI [4.03, 6.57], corrected $P < 0.05$), relative to baseline rates in each region.

Sleep Spindles Coordinate Across Distant Brain Regions and Are Modulated by OFC Slow Oscillations. Controlling for baseline rates, we evaluated the incidence of detected spindle onsets in each region relative to the OFC slow oscillation downstate trough (*Methods*). We found that spindle incidence in each region was modulated by OFC slow oscillations (Fig. 2*B*). Spindles in the

thalamus were maximally up-regulated 0.125 s (0.025 s bins) after the OFC slow oscillation trough (by a factor of 1.67, 95% CI [1.52, 1.8], corrected $P < 0.05$). Spindles in the medial orbitofrontal cortex were maximally up-regulated 0.275 s after the OFC slow oscillation trough (by a factor of 1.26, 95% CI [1.18, 1.34], corrected $P < 0.05$). Spindles in the hippocampus were maximally up-regulated 0.225 s after the OFC slow oscillation trough (by a factor of 1.29, 95% CI [1.19, 1.39], corrected $P < 0.05$). Compared to spindle onsets, the maximum spindle amplitude in each region aligned with the slow oscillation up-state in the thalamus (0.5 s after the OFC slow oscillation trough), the hippocampus (0.8 s), and the OFC (1 s; see Fig. 2*B* triangles and *SI Appendix*, Fig. S1*A*), as expected. To confirm that our results were not due to the specific slow oscillation phase that anchored our analysis, we evaluated detected spindle incidence modulation (using the onset of spindles) referenced to the positive-to-negative zero-crossing prior to the slow oscillation trough and found consistent results (*SI Appendix*, Fig. S1 *B* and *C*).

Sleep spindles in all three regions were also moderately—but significantly—up-regulated prior to the OFC slow oscillation trough, coinciding with the first up-state of the triphasic OFC slow oscillation (Fig. 2*B*). In the OFC, the maximum up-regulation of spindle incidence occurred 1.125 s before the OFC slow oscillation trough (increase by a factor of 1.11, 95% CI [1.07, 1.15], corrected $P < 0.05$). In the thalamus, the maximum up-regulation of spindle incidence occurred 1.225 s before the OFC slow oscillation trough (increase by a factor of 1.16, 95% CI [1.11, 1.21], corrected $P < 0.05$). In the hippocampus, the maximum up-regulation of spindle incidence occurred 1.275 s before the OFC slow oscillation trough (by a factor of 1.09, 95% CI [1.06, 1.12], corrected $P < 0.05$). Early spindle activity preceding the slow oscillation trough and coinciding with the first slow oscillation up-state was also observed when only isolated slow oscillations (separated by at least ±3 s from another slow oscillation) were evaluated (*SI Appendix*, Fig. S2).

Thalamic sleep spindles had higher amplitude (mean 4.9 μV, SE 0.18 μV) and duration (mean 1.24 s, SE 0.07 s) than hippocampal spindles (amplitude mean 3.55 μV, SE 0.14 μV, t(25) = 8.47, P = 8.2e-9; duration mean 0.97 s, SE 0.07 s, t(25) = 6.14, P = 2e-6) and higher amplitude but not duration than OFC spindles (amplitude mean 3.65 μV, SE 0.15 μV, t(25) = 7.45, P = 8.3e-8; duration mean 1.15 s, SE 0.09 s, t(25) = 1.38, P = 0.18). OFC sleep spindles had a lower mean frequency (11.9 Hz, SE = 0.07 Hz) than spindles detected in the hippocampus (mean 12.25 Hz, SE 0.08 Hz, t(25) = 3.95, P = 5.7e-4). In the thalamus, spindle frequency varied across nuclei; spindle frequencies were slower in the anterior nucleus than in the pulvinar nucleus (11.99 Hz vs. 12.9 Hz, t(26) = –4.27, P = 4.6e-4). The timing of slow (9 to 12 Hz) and fast (12 to 15 Hz) spindle modulation relative to the OFC slow oscillation was similar across brain regions (*SI Appendix*, Fig. S3).

To evaluate the impact of co-occurring thalamic spindles and OFC slow oscillations on spindle propagation, we evaluated the incidence of cortical or hippocampal spindles in the setting of thalamic spindles with and without a co-occurring OFC slow oscillation. When a thalamic spindle and orbitofrontal slow oscillation were both present, OFC spindle occurrence increased by a factor of 2.76 (95% CI [2.56, 2.93], corrected $P < 0.05$) and hippocampal spindle occurrence increased by a factor of 2.56 (95% CI [2.35, 2.76], corrected $P < 0.05$). In contrast, in the absence of a co-occurring OFC slow oscillation, a thalamic spindle up-regulated spindle occurrence in the OFC by a factor of 1.86 (95% CI [1.62, 2.08], corrected $P < 0.05$) and in the hippocampus by a factor of 1.62 (95% CI [1.43, 1.79], corrected $P < 0.05$).

Ripple Oscillations Coordinate Across Distant Brain Regions and Are Modulated by OFC Slow Oscillations. Sharp wave ripples, characterized by fast 80 to 120 Hz oscillations lasting less than 100 ms occurring alongside a 2 to 8 Hz wave, have classically been described in the hippocampus (44). Recently, ripple oscillations detected agnostic to sharp waves have also been reported in the thalamus and cortex (12, 17, 45, 46). Controlling for baseline rates, we evaluated the ripple incidence in each region relative to the OFC slow oscillation downstate trough (*Methods*). We found that ripple incidence in each region was modulated by an OFC slow oscillation (Fig. 2*C*). Ripples in the medial orbitofrontal cortex were maximally up-regulated 0.425 s after the OFC slow oscillation trough (by a factor of 1.34, 95% CI [1.18, 1.51], corrected $P < 0.05$). Ripples in the thalamus were maximally up-regulated 0.15 s after the OFC slow oscillation trough (by a factor of 1.45, 95% CI [1.35, 1.54], corrected $P < 0.05$). Ripples in the hippocampus were maximally up-regulated 0.5 s after the OFC slow oscillation trough (by a factor of 1.09, 95% CI [0.99, 1.2], corrected $P = 0.09$). Ripple incidence modulation remained consistent but shifted forward in time when referenced to the positive-to-negative zero-crossing prior to the slow oscillation trough (*SI Appendix*, Fig. S1*C*).

Ripples in the hippocampus, but not the OFC or thalamus, were up-regulated prior to the OFC slow oscillation trough. The incidence of hippocampal ripples was increased 0.9 s before the slow oscillation trough (by a factor of 1.10, 95% CI [1.04, 1.16], corrected $P < 0.05$), concordant with the first slow-oscillation up-state and increase in hippocampal sleep spindles (Fig. 2*B*). Early ripple activity, preceding the slow oscillation trough and coinciding with the first slow oscillation peak, was also observed when only isolated slow oscillations (separated by at least ±3 s from another slow oscillation) were evaluated (*SI Appendix*, Fig. S2).

Although ripples were detected in each location, we found that ripples in the hippocampus had higher amplitudes (13.99 uV, s.e. 1.72 μV) compared to those detected in the thalamus (3.34 μV, SE 0.94 μV, t(25) = 5.71, P = 5.9e-6) or orbitofrontal cortex (4.51, SE 0.77 μV, t(25) = 5.19, P = 2.3e-5). We also found that ripples in the hippocampus had longer durations (43.85 ms, SE 0.78 ms) than those detected in the thalamus (37.2 ms, SE 1.0 ms, t(25) = 5.08, P = 3.1e-5), but no evidence of a difference in ripple durations between the hippocampus and orbitofrontal cortex (41.6 ms, SE 1.9 ms, t(25) = 1.1, P = 0.28). Ripples detected in the thalamus were higher frequency oscillations (93.0 Hz, SE 0.3 Hz) compared to those detected in the hippocampus (85.6 Hz, SE 0.3 Hz, t(25) = 18.81, P = 2.9e-16) or OFC (86.8 Hz, SE 0.53 Hz, t(25) = 11.38, P = 2.2e-11). Distributions for all characteristics are shown in *SI Appendix*, Fig. S4.

Coordination of Sleep Oscillations Across Distant Brain Regions Supports Motor Memory Consolidation. To investigate whether the coupling of sleep oscillations across regions predicts overnight motor consolidation and identify the cross-regional and cross-frequency circuits that support it, we trained eligible subjects on the motor sequence typing task (MST). Several previous studies have demonstrated that gains in offline MST performance can be predicted by the rate of oscillations linked to memory consolidation—slow-oscillations, spindles and ripples (35, 40, 42). In total, 14 subjects completed the task (5 with bilateral sampling). In most subjects (9/14), cross-frequency and cross-regional sleep oscillation couplings were computed for the one recorded hemisphere and compared to MST task performance of the contralateral hand. In 5 subjects with SEEG recordings from both hemispheres, the electrophysiological features were

averaged across hemispheres and compared to average MST task performance across hands.

The rates of each sleep oscillation in each region, the rates of coupling of each sleep oscillation combination (i.e., slow oscillation-spindle, slow oscillation-ripple, spindle-ripple, slow oscillation-spindle-ripple) within each region, and the rates of coupling of each sleep oscillation combination across each region were computed (40 rates in total, see *Methods* and Fig. 3). This first round of analyses excluded sleep oscillations that co-occurred with epileptic activity in any region. We analyzed the correlation between each of these 40 combinations of sleep oscillations (uncoupled and coupled, within and across brain regions) and performance change on the motor sequence typing task. In this univariate analysis, the rate of sleep oscillations correlated positively with overnight MST performance change for 36/40 predictors (Fig. 4*A*). Significant correlations (uncorrected permutation tests, $P < 0.05$, see *Methods*) were found between overnight MST performance change and hippocampal–OFC–coupled ripple rate ($r = 0.54$), hippocampal slow oscillation-ripple coupling rate ($r = 0.54$), hippocampal ripple rate ($r = 0.47$), and OFC slow oscillation -hippocampal ripple coupling rate ($r = 0.47$). These results indicate a consistent presence of ripples among the significant positive correlations with overnight MST performance change.

Co-occurrence of Epileptic Activity with Sleep Oscillations Across Distant Brain Regions Disrupts Motor Memory Consolidation. As all subjects included had drug refractory epilepsy, we were also able to investigate the impact of epileptic activity on overnight MST performance change. To do so, we detected epileptic spikes during N2 and N3 sleep using an automated epileptic spike detector (*Methods*). We found that the rate of sleep oscillations with coupled epileptic spikes correlated negatively with overnight MST performance change for 30/40 predictors (Fig. 4*B*). Significant correlations (uncorrected permutation tests, $P < 0.05$, see *Methods*)

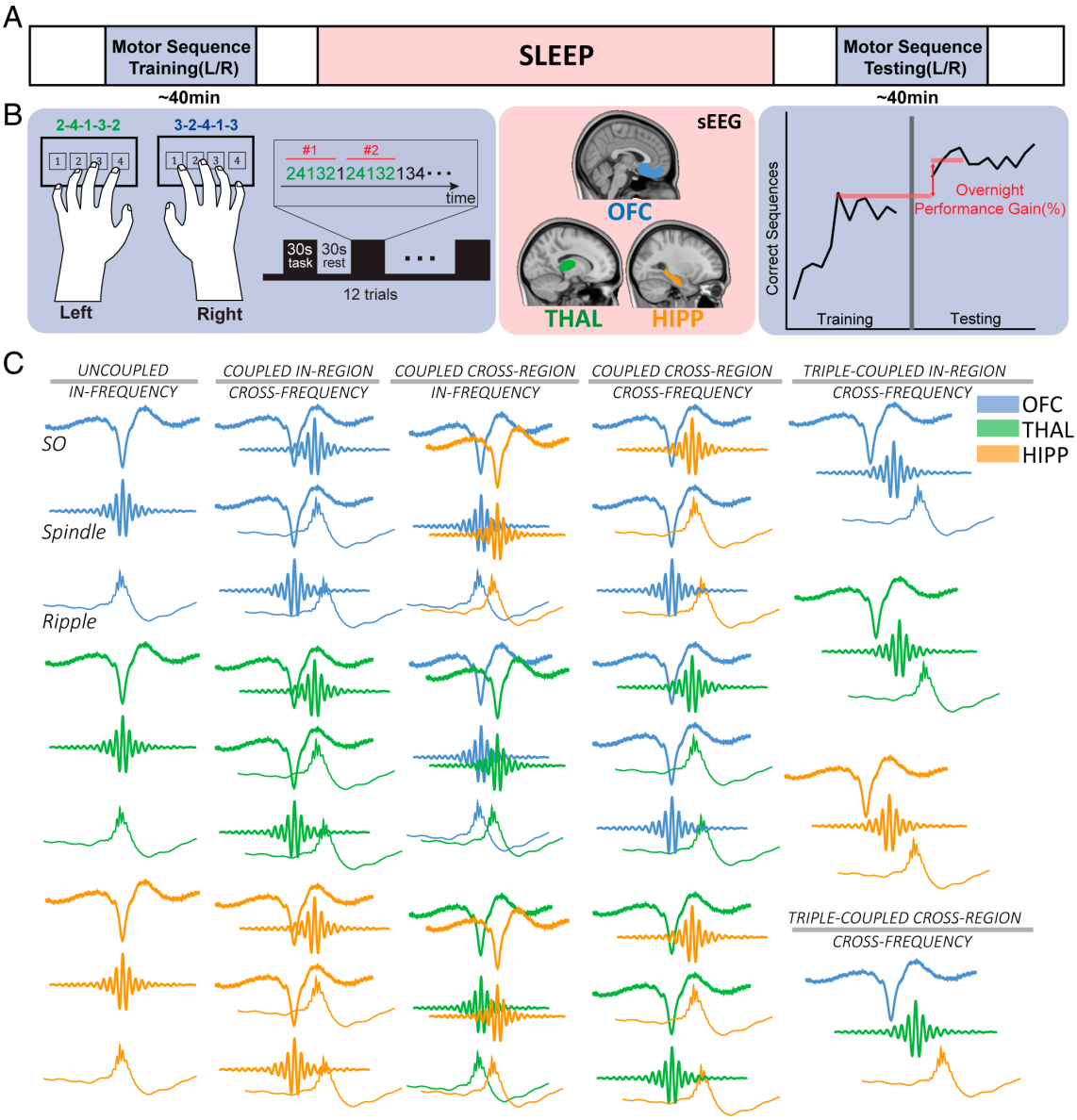

Fig. 3. Cross-frequency and cross-regional sleep oscillations that predict motor memory consolidation. (*A* and *B*) To estimate sleep-dependent memory consolidation, subjects typed a 5-digit sequence quickly and accurately for twelve 30 s trials with each hand before sleep. Neurophysiological recordings were obtained during sleep. After sleep, subjects were tested on the motor sequence task (MST). (*C*) During stages 2 and 3 non–rapid eye movement sleep the rates of slow oscillations, sleep spindles, and ripples; all pairwise combinations of these oscillations within and across regions; and triple-coupling within and across regions were used as predictors to model overnight MST performance change.

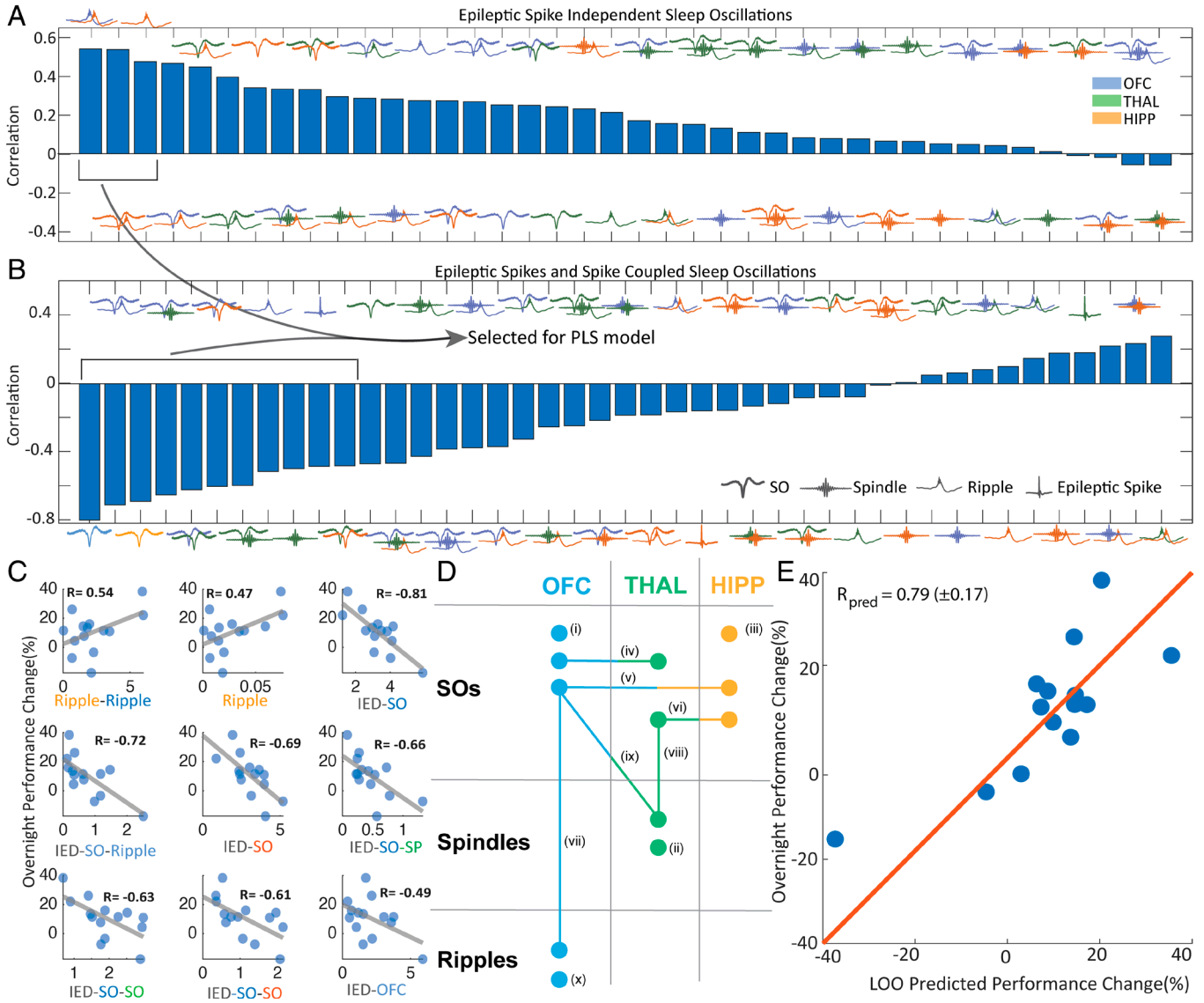

Fig. 4. Sleep oscillations predict improved memory consolidation, unless coupled to epileptic spikes. (*A* and *B*) Univariate correlations between rates of sleep oscillation predictors (*A*) uncoupled or (*B*) coupled to epileptic spikes and overnight performance change. Symbols centered on each tick mark indicate the rhythmic feature (SO, spindle, ripple, or epileptic spike) and colors indicate the brain region (blue—orbitofrontal cortex; green—thalamus; orange—hippocampus); see legend. (*C*) Individual scatterplots of a subset of selected predictors with overnight MST performance change. (*D*) Illustration of the 10 epileptic spike coupled sleep oscillation rates negatively correlated with memory consolidation and included in the partial least squares model were SOs occurring in (i) OFC and (iii) hippocampus, (ii) spindles occurring in thalamus, SOs co-occurring in (iv) OFC–thalamus, (v) OFC–hippocampus, and (vi) thalamus–hippocampus; (vii) SOs co-occurring with ripples in OFC, and (viii) SOs co-occurring with spindles in thalamus; (ix) SOs in OFC co-occurring with thalamic spindles, and (x) ripples in OFC. (*E*) Prediction of overnight change in MST performance using a partial least squares (PLS) derived model versus the observed overnight performance change. Each point indicates data from one subject, and the line indicates equality. R_{pred} is predictive correlation from leave-one-out (LOO) cross-validation.

were found for epileptic-spike-coupled slow oscillation rates in the OFC (r = −0.81), hippocampus (r = −0.70), and thalamus (r = −0.47), as well as for epileptic spikes coupled to co-occurring slow oscillations across regions: OFC and thalamus (r = −0.63), OFC and hippocampus (r = −0.61), and thalamus and hippocampus (r = −0.48). In the OFC, epileptic-spike-coupled ripple rates (r = −0.52) and SO-ripple rates (r = −0.72) showed strong negative correlations with MST performance change. Two additional significant correlations included thalamic spindles: epileptic-spike-coupled thalamic slow oscillation-spindle rates (r = −0.60) and epileptic-spike-coupled OFC slow oscillation-thalamic spindle rates (r = −0.66). Finally, epileptic spikes coupled to triple coupling across the cortex (slow oscillation), thalamus (spindle), and hippocampus (ripple) showed a significant negative correlation (r = −0.47). Thus, across predictors, the significant negative correlations consistently involved epileptic spikes co-occurring with at least slow oscillations (Fig. 4*C*). Epileptic spike rate alone, in contrast, was inconsistently correlated with memory across regions, with only OFC epileptic spike rate (r = −0.49) showing a significant negative relationship to MST performance change.

Optimal Predictors of Sleep-Dependent Motor Memory Consolidation in Epilepsy. To identify the optimal predictors for MST performance change from the 83 assessed individual and coordinated sleep oscillation rates, we first identified predictors that consistently covaried with MST performance change across subjects in a leave-one-out predictor selection procedure (*Methods*; Fig. 4 *A* and *B*). Of the 83 original predictors, a subset of 14 predictors were selected. This subset included three positive predictors: the rate of ripples co-occurring in the hippocampus

and OFC (without epileptic spikes), the rate of hippocampal ripples, and the rate of hippocampal slow oscillation-coupled ripples. The remaining 11 predictors that negatively correlated with performance change included OFC epileptic spike rate and 10 sleep oscillations with co-occurring epileptic spikes, where 8 of these predictors included slow oscillations coupled with epileptic spikes (Fig. 4 *C* and *D*).

Applying partial least squares regression (*Methods*) to these 14 predictors, we found that the model explained 62% of the variance in overnight motor performance change across subjects (leave-one-out cross-validation predictive R = 0.79, SE 0.17, P = 2e-6; Fig. 4*E*). Controlling for the influence of epileptic spike rates on the predictors (*Methods*), we found that the resulting model still explained 41% of the variance (*SI Appendix*, Fig. S6), demonstrating that epileptic spikes co-occurring with sleep oscillations are more impactful on memory consolidation than epileptic spikes occurring in isolation. Consistent with this result, after controlling for epileptic spike rates, the feature-level correlations to motor performance change retained a systematic relationship with the original, unadjusted correlations (R = 0.71, P = 2e-7, *SI Appendix*, Fig. S6). We conclude that coordinated sleep oscillations across the OFC, thalamus, and hippocampus support motor memory consolidation and that epileptic spikes coupled to these rhythms interfere with this process.

Conceptual Model of the Hierarchical Coordination of Sleep Oscillations Supporting Memory Consolidation. Our findings support a model in which slow oscillations in the orbitofrontal cortex serve as primary organizers of network oscillatory activity during stages 2 and 3 non–rapid eye movement sleep. Slow oscillations show a consistent temporal ordering across the OFC, thalamus, and hippocampus, which aligns with traveling-wave-like dynamics or with local oscillatory generators coordinated by reciprocal connections or a common drive. In the thalamus, the slow oscillation facilitates thalamocortical and/or thalamo-hippocampal spindles during the down-to-upstate transition. The slow oscillation up-state also comodulates and coordinates hippocampal and orbitofrontal ripples. This orchestrated cascade of activity across the network is graphically represented in Fig. 5*A*.

Conceptual Model of Sleep-Dependent Memory Impairment in Epilepsy. Our findings suggest a model in which memory impairment in epilepsy results from the interference of coordinated sleep oscillations by co-occurring epileptic spikes. Although slow oscillations normally orchestrate memory consolidation through spindle and ripple facilitation, in epilepsy, slow oscillations can also facilitate epileptic spikes on the initial up-state (9, 47). As observed in rodent models, when an epileptic spike is coupled to a slow oscillation, it can hijack (26, 34) this foundational oscillatory event and interfere with the downstream physiological cascade. Notably, rates of epileptic spikes coupled to slow oscillations were among the most consistent negative predictors of overnight motor performance change. This disrupted oscillatory cascade is illustrated in Fig. 5*B*.

Discussion

In this manuscript, we show a hierarchical coordination of sleep oscillations that supports human motor memory consolidation and that epileptic spikes can hijack this process to impair memory in epilepsy. Orbitofrontal slow oscillations modulate a cross-regional cascade of oscillations in which the downstream rate of hippocampal ripples—coupled to orbitofrontal ripples or alone—predicts successful overnight MST performance change. Critically,

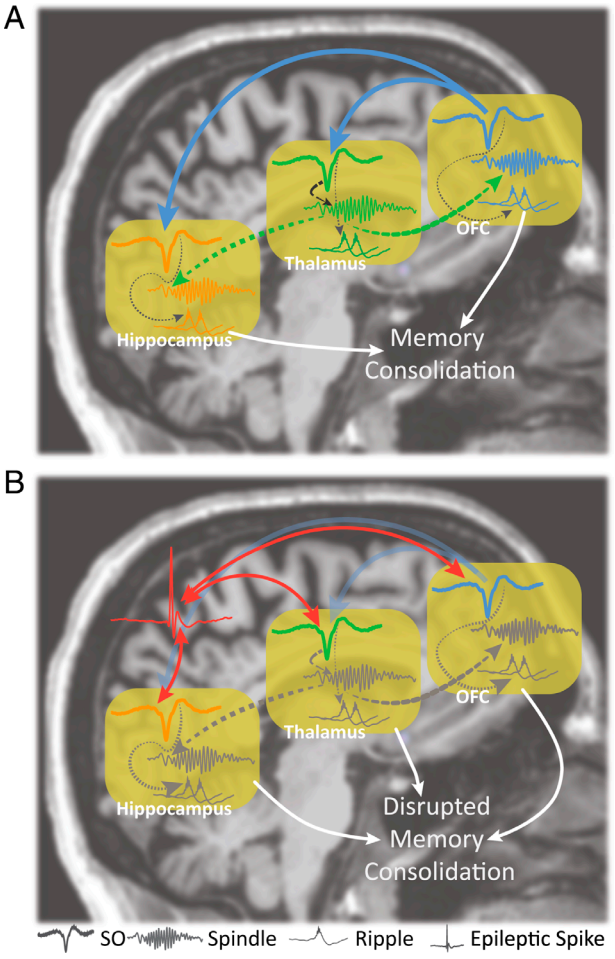

Fig. 5. The hierarchical cascade of sleep oscillations underlying memory consolidation and their disruption in epilepsy. (*A*) Slow oscillations show a temporal ordering, presenting first in the orbitofrontal cortex, then thalamus and hippocampus (blue arrows). Slow oscillations facilitate spindles during the down-to-upstate transition (black arrow), which are coordinated between the thalamus and both the cortex and hippocampus (green arrows). Slow oscillations also facilitate ripples during the up-state (dotted gray arrows). Ripples coordinated across the hippocampus and frontal cortex maximally facilitate overnight memory consolidation (white arrows). (*B*) Epileptic spikes coupled to slow oscillations (red arrows) interfere with memory consolidation, potentially by corrupting the information transfer supported by this hierarchical cascade of sleep rhythms.

the coupling of epileptic spikes to sleep oscillations, especially slow oscillations, interferes with this overnight behavioral change.

The sequential pattern we observed, whereby orbitofrontal slow oscillations modulate thalamic spindles and hippocampal ripples, supports the established framework proposed for systems memory consolidation (15, 16, 48). In this framework, slow oscillations create windows of excitability, spindles facilitate plasticity, and ripples reactivate or "replay" action potential sequences to enable cross-regional synaptic strengthening for long term memory storage. Our data are consistent with observations that slow oscillations initiate in the frontal cortex (5, 6) to organize widespread activation across the thalamus and hippocampus. Further, our finding that coupled hippocampal and orbitofrontal ripples are strong positive predictors of memory consolidation is consistent with prior observations that hippocampal replay is directed toward the orbitofrontal cortex for integration and long-term storage (1, 12, 17). Additionally, we found a modest up-regulation of thalamic spindles and hippocampal ripples preceding the first slow oscillation up-state, also noted by others (17, 49, 50). As this could indicate a preparatory or bidirectional information flow, these

subtle temporal dynamics require further investigation, potentially through interventional studies.

A key finding of our study is that the negative impact of epileptic spikes on memory is not explained solely by the overall burden of epileptic spikes, but predominantly by the rate at which epileptic spikes are coupled to critical sleep oscillations. Interactions between epileptic spikes and sleep oscillations have been recognized as a significant factor in the memory impairment seen in epilepsy (9, 32, 34, 47, 51–53). We find that epileptic spikes, coupled with slow oscillations in any of the regions studied were strong negative predictors of overnight motor memory consolidation. As slow oscillations orchestrate the cross-regional slow-oscillation-spindle-ripple cascade, spikes interfering with the foundation of this hierarchy could prevent (9, 31, 51) or distort (51, 54, 55) the intended information transfer typically supported by spindles and ripples. Cortical and subcortical excitability are known to be elevated in epilepsy (56), which may increase the rates of epileptic spikes and sleep oscillations and, therefore, the chance-level occurrence of epileptic-spike-sleep-oscillation coupling. However, prior studies indicate that sleep oscillations are decreased in epilepsy (9, 34, 35). Further, after accounting for the influence of epileptic spike rates, epileptic spikes coupled to sleep oscillations remained strong predictors of motor performance change in our data. These results suggest a potential therapeutic direction to improve memory function in epilepsy is to decouple spikes from slow oscillations.

Ripples and ripple-associated replay have classically been associated with the unique architecture and function of the hippocampus (44). However, evidence now exists that the neocortex and the thalamus produce discrete bursts of fast oscillations that approximate hippocampal ripple morphologies and, at least in the neocortex, can show similar replay (12, 13, 46). We identified ripples in the hippocampus, cortex, and thalamus with distinct morphological features (i.e., duration, amplitude, and frequency). However, these morphological differences alone are insufficient to clarify the potential functional difference. These ripple-like events in the thalamus and neocortex also coupled strongly with slow oscillations and spindles. Our work supports prior findings in rodent models that sleep oscillations in the prefrontal-cortex and hippocampus may uniquely facilitate targeted reactivation and strengthening of specific memory engrams (23, 57).

Spike-independent triple-coupling of slow oscillations, spindles, and ripples was not selected in our analysis to predict overnight motor performance change. This result suggests that the hierarchical cascade of sleep oscillations may primarily function, with respect to systems memory consolidation, to facilitate ripples, which did predict overnight performance change. In contrast, triple-coupling that co-occurred with epileptic spikes was associated with worse memory, while we did not identify a relationship between spike-coupled hippocampal ripples and performance change. This finding suggests that, when present in the full cascade of triple-coupled oscillations, epileptic spikes may expand, scramble, or distort replay and memory processes more than an epileptic spike can on a focal ripple alone (26, 29, 30, 32, 58–61). Alternatively, an epileptic spike coupled to a slow oscillation may hijack the circuit and prevent downstream spindles or ripples from occurring (9).

The MST used in this study engages procedural memory. The MST corresponds to functional activation of the hippocampus and frontal cortex (62, 63) and benefits from sleep-dependent consolidation, potentially via ripple-mediated replay (2, 38). Indeed, we observed that hippocampal–orbitofrontal cortex ripple coupling positively predicted overnight MST performance change, possibly reflecting the consolidation of spatial or sequential aspects of this task (38). However, whether offline changes in MST performance reflect memory enhancement remains debated, and sleep oscillations may preferentially stabilize performance rather than improve it (64, 65). While MST served as a robust assay for the network dynamics of motor memory, intracranial human signals (ripples, high-frequency activity, and single-neuron activity) have been linked to multiple memory domains, including episodic verbal retrieval and replay (14), spatial memory (66), associative memory (67), semantic/autobiographical memory (68), and temporal organization of episodic memories (69). Thus, future work should investigate whether the observed coordination and disruption patterns in sleep also generalize to these other domains of memory.

Our findings are based on recordings from patients with epilepsy. While these data enable a unique opportunity to observe widespread brain dynamics and probe the impact of epileptic disruptions on sleep oscillations and memory, patients with epilepsy also have a range of neurophysiological abnormalities. Despite the disparate epilepsy etiologies evaluated, we saw consistent relationships between sleep oscillations and memory, as has previously been reported in both patients with epilepsy and controls (34, 35). Further, the predictive model we report here requires confirmation in larger, independent cohorts. Future work exploring oscillatory coordination across different sleep stages, early versus late sleep, and the contributions of additional brain regions linked to procedural memory, such as the striatum, will provide a more complete picture. Investigating the precise timing of epileptic spikes within the slow-oscillation cycle and their relationship to subsequent spindle and ripple activity could offer deeper mechanistic insights.

In our analyses, coupling is measured as event-level temporal coordination or co-occurrence within and across different recording sites. This metric does not make a claim on phase synchronization between continuous oscillations but does not preclude it. Accordingly, the present framework captures cross-regional coordination but does not uniquely determine whether the observed relationships arise from a single distributed generator expressed across sites or from locally generated oscillatory bursts whose timing is aligned by common input or reciprocal interactions. While bipolar referencing, unique regional characteristics, and systematic nonzero lags argue for locally generated bursts rather than volume conduction (43), definitively adjudicating generator structure and directionality will require higher-density sampling, biophysical source modeling, and/or causal perturbation. We note that the temporal ordering of slow oscillations across regions was consistent regardless of whether the downstate trough or the preceding zero-crossing was used as the reference point, though the trough provided more stable delay estimates, likely due to regional differences in slow oscillation waveform morphology (5, 70). Measures of individual events inevitably combine signal and noise, yielding potential false-positive and false-negative detections. However, we found no temporal modulation of false spindle or ripple detections around slow oscillations in simulated noise (see *SI Appendix*, Fig. S7), indicating that the coupling structure we observe in human data is not an artifact of detection from aperiodic activity (71). Nonetheless, while these existing detection methods perform adequately here and in other studies (18, 34, 35, 40, 72), future work can further justify and optimize these event detection techniques.

In conclusion, our findings reveal a complex interplay of sleep oscillations across the orbitofrontal cortex, thalamus, and hippocampus that supports motor memory consolidation. Epileptic spikes coupled to this oscillatory cascade interfere with motor

memory consolidation and highlight one mechanism by which epileptic activity can impair cognition in patients with epilepsy. These results deepen our understanding of systems-level memory consolidation and identify candidate mechanisms to target when developing treatments for memory dysfunction in epilepsy.

Methods

Subject Data Collection. We prospectively recruited patients undergoing clinical evaluation for drug-resistant epilepsy at Massachusetts General Hospital who had simultaneous stereo-electroencephalography (sEEG) recordings from the medial orbitofrontal cortex (OFC), thalamus, and hippocampus, along with scalp EEG. The orbitofrontal cortex was selected due to its dense recurrent connectivity with the hippocampus (73) and thalamus (74–76), as well as its role in processes of memory (77). All patients provided informed consent, and the study was approved by the Massachusetts General Hospital Institutional Review Board.

Electrode localization was performed using pre- and postoperative high-resolution MRI scans coregistered with postimplantation CT scans. We first visually assessed the gross electrode positions in the medial orbitofrontal cortex, thalamus, and hippocampus of sEEG electrodes for which these areas were the intended targets during surgical placement. To refine localization, we analyzed the electrophysiological signals along each electrode shaft, identifying transitions into white matter by noting sharp reductions in signal amplitude. This two-step approach allowed for improved anatomical localization of recording sites. Specific thalamic and hippocampal subregions sampled for each subject are detailed in *SI Appendix*, Table S2.

EEG Data Collection, Preprocessing, and Channel Selection. Intracranial EEG data were collected using the clinical Natus Quantum system (Natus Neurology Inc., Middleton, WI). Depth electrodes (PMT Depthalon depth platinum electrodes with 3.5 mm spacing, 2 mm contacts, and 0.8 mm diameter; or AdTech depth platinum electrodes with 5–8 mm spacing, 2.41 mm contact size, and 1.12 mm diameter) were placed in the regions of clinical interest and sampled at 1,024 Hz. Using only intracranial electrophysiology, we sleep staged based on a validated algorithm that was intended for use in patients with epilepsy (78). This algorithm has shown 85% accuracy at detecting non–rapid eye movement sleep stages using slow oscillation and spindle activity across electrodes. We analyzed only non-REM stage two and stage three sleep segments (N2 and N3) for analysis (mean 276 min, minimum 146.5 min, maximum 438.5 min). All N2 and N3 sleep segments over one night were concatenated for analysis.

For slow oscillation detections, we used all electrodes from the medial OFC, thalamus, and hippocampus with a midline, far-field noncephalic reference over the second cortical spinous process. For spindle, ripple, and epileptic spike detections, we examined adjacent medial OFC, thalamic, and hippocampal depth electrodes in a bipolar reference. We applied bipolar referencing for improved spatial and temporal resolution for these higher frequency, spatially localized oscillations.

Epileptic Spike Detection. To detect epileptic spikes, we used a previously developed method (9, 79). First, we bandpass filtered the data both forward and backward using a finite impulse response (FIR) filter between 25 to 80 Hz (MATLAB function *filtfilt*). We then applied a Hilbert transform, calculated the analytic signal, and the amplitude envelope of this signal. For each voltage signal, the moments when the amplitude envelope exceeded three times the mean amplitude were identified as candidate spikes. To ensure the candidate spikes were not due to gamma-band oscillatory bursts or spindles, we also calculated the regularity of oscillations in an interval (±0.25 s for gamma, ±0.3125 s for spindles) around each candidate spike. To assess the regularity of the signal in this interval, we computed the Fano factor (80) estimated by i) detrending the interval of unfiltered data at each candidate spike, ii) identifying peaks and troughs after limiting maximum delays between extrema (between peaks or between troughs) to 1/50 s for gamma-band oscillatory bursts or 1/20 s for spindles, iii) calculating the interpeak and intertrough intervals, and iv) estimating the ratio of the variance of the interpeak and intertrough intervals to the mean of the interpeak and intertrough intervals. We then removed candidate spikes if the maximum deviation (calculated by rectifying the data and identifying the maximum voltage) of the unfiltered data was below three times the mean amplitude or if the Fano factor was less than 2.5 for gamma-band oscillatory bursts or less than 5 for spindles. We additionally required that the candidate spike peak was at least twice the value of the nearest neighboring peak. Of the resulting spikes, those detected within 20 ms of one another were merged into a single spike detection. We visually examined individual detections and the averaged spike waveform for each subject to confirm that the method accurately detected epileptic spikes in cortical, hippocampal, and thalamic recordings. We show example averaged spike waveforms and the time-frequency spectrogram in *SI Appendix*, Fig. S5.

Slow Oscillation Detection. We applied a method consistent with prior publications (9, 15, 20, 72) to capture the 0.75 to 1 Hz range of slow oscillations. Briefly, slow oscillations were detected by i) filtering the data (both backward and forward) into the 0.4 to 4 Hz band using a FIR filter (4092 order); ii) identifying all negative to positive zero-crossings and the time interval t between subsequent negative to positive zero-crossings; iii) retaining all time intervals of duration $0.75\ s \leq t \leq 3\ s$ (corresponding to oscillations between ~0.4 to 1.33 Hz, due to filtering) and identifying the negative peak and peak-to-peak amplitude; iv) omitting intervals in the bottom 75th percentile of peak-to-peak amplitude and detections with peak greater than 1,000 μV or trough less than −1,000 μV; v) retaining any remaining intervals as slow oscillations. When estimating the cross-correlation histograms, we omitted slow oscillations that co-occurred with an epileptic spike within 0.5 s prior to the downstate and 1 s after the downstate [based on results from Wodeyar et al. (9)].

Spindle Detection. We applied an existing spindle detector with robustness to epileptic spikes and sharp transients (34). The spindle detector estimates a latent state–the probability of a spindle–using three features: the Fano factor (estimated for data FIR filtered between 3 and 25 Hz), normalized power in the spindle band (9 and 15 Hz), and normalized power in the theta band (4 and 8 Hz). Distributions of expected values for these parameters were determined using manually detected spindles in the scalp EEG of subjects with sleep-activated spikes. The spindle detector estimates the probability of a spindle in 0.5 s intervals (0.4 s overlap). We detected a spindle when the probability crossed 0.95, chosen by optimizing the sensitivity and specificity of the detector. We retained spindles with a minimum duration of 0.5 s, a maximum duration of 5 s, and separated by at least 0.5 s; spindles within 0.5 s of one another were merged into a single spindle detection. We visually confirmed that the method accurately detected sleep spindles in OFC, hippocampal, and thalamic recordings and omitted all spindles that had a co-occurring spike within the spindle duration for cross-correlation histogram analysis.

We estimated spindle frequencies following a method similar to that proposed in Kwon et al. (81). To do so, we i) ensured each spindle reached duration 10 s; ii) applied a Hanning taper; iii) computed the spectrum; iv) removed from the spectrum the 1/f-like background estimated between 4 and 50 Hz; v) determined the frequency of maximum power between 9 and 15 Hz in the resulting spectrum. We repeated this process for all detected spindles.

Ripple Detection. We detected ripples using a validated method adapted from Staba et al. (82) and applied in several studies (18, 40). For a given bipolar signal, we i) bandpass filtered the signal between 70 and 150 Hz; ii) applied the Hilbert transform to compute the ripple-band envelope; iii) estimated the RMS amplitude of the ripple-band envelope and set the threshold for ripple detection at the 97.5th percentile, similar to that used in other studies (20, 40, 83); iv) retained ripples that exceeded the 97.5th envelope threshold for at least 6 ms, produced at least 6 voltage peaks in both the raw and the bandpass filtered signal, and possessed a ripple-band envelope >3 SDs above the mean for all values in a 200 ms interval centered on the ripple-band envelope peak. For the cross-correlation histogram analysis, we omitted ripples that co-occurred with a spike within 0.5 s. Ripple spectrograms computed using a multitaper spectral estimate with 2 Hz bins, standardized within subject, and averaged across subjects are shown in *SI Appendix*, Fig. S4.

Temporal Coupling Estimates. We estimate cross-regional and cross-frequency relationships using event-based covariance statistics, specifically the normalized cross-correlation histogram (9). In this approach, we use event detections to estimate relationships between regions and oscillations, thus minimizing bias from interictal activity in the original SEEG data. Throughout this manuscript, coupling refers to the temporal co-occurrence of events within and across different

recording sites, not necessarily to phase synchronization between continuous oscillations. For each slow oscillation detection, we assigned the event time to the downstate trough. For each spindle detection, we assigned the event time to either the spindle start time or the maximum amplitude moment depending on the analysis performed. For each ripple detection, we assigned the event time to the moment of maximum amplitude. We compute the cross-correlation histogram between two rhythms (oscillation$_1$ and oscillation$_2$) in two regions (region$_1$ and region$_2$) as follows: i) create binary time series for each region, marking the event times of oscillation$_1$ in region$_1$ and oscillation$_2$ in region$_2$; ii) determine the time t_i of each event i from the binary time series of oscillation$_1$ in region$_1$; iii) compute the delays between all events in the binary time series from oscillation$_2$ in region$_2$ within $\pm$ 3 s s of each t_i. These delays for all channel pairs in the two regions within each subject were computed.

To estimate the population-level distribution of event incidence around slow oscillation downstate troughs, we employed the following bootstrapping approach: i) For every iteration of the bootstrap, we sampled randomly with replacement from all hemispheres of all subjects to select 26 hemispheres and concatenated all delays relative to downstate trough event detections from each selected hemisphere. ii) We generated a smoothed estimate of the histogram of the resampled delays using 75 ms kernel smoothing (MATLAB *fitdist*). iii) We calculated the histogram in 25 ms intervals from −3 to +3 s relative to a slow oscillation downstate trough. We repeated the entire procedure 100 times to generate 100 resampled histograms yielding a sampling distribution for the lag histogram. We then calculated the up or down-regulation of event occurrences by dividing the histogram between [−2,2] s by the average of the histogram in the −2.8 to −2 s and 2 to 2.8 s intervals (avoiding edge effects from normalization). This approach yields a modulation value for time bins between [−2, 2] s that can be interpreted as the multiplicative factor applied to the average event rates of the oscillation over the [−2.8, −2] s and [2, 2.8] s intervals. The mean and SE of the normalized histogram were estimated. We repeated the procedure above to assess temporal relationships between slow oscillations across regions, between OFC slow oscillations and spindles across regions, and between OFC slow oscillations and ripples across regions. Separately, we calculated the total number of events using unnormalized histograms with 25 ms time bins, summing across all subjects.

To assess the contamination of co-occurring events by noise, we simulated 3 h of pink noise ($1/f^{\alpha}$ with $\alpha = 1$) representing activity from three channels during NREM sleep periods for one night and repeated this 26 times (reflecting the sample size). We then applied the previously described detectors to identify slow oscillations (mean = 5.08/min, SE = 0.01), spindles (mean = 3.57, SE = 0.03), and ripples (mean = 0.46, SE = 0.01). Although the percentile-based thresholding ensures nonzero detections of events even for pink noise, our application of the method discussed above to estimate normalized lag histograms revealed a uniform and limited pattern of co-occurrence around slow oscillations (*SI Appendix*, Fig. S7). This result suggests that the modulation in spindle or ripple event rates around slow oscillations is not driven by aperiodic noise (71).

Finger Tapping MST. For the behavioral task, we used the finger tapping MST (37), a widely used assay in sleep research on procedural learning. This task is expected to capture sleep-dependent motor memory consolidation or stabilization (38, 64) in healthy adults, where performance improves or remains stable after sleep compared to an equal period of wakefulness. Subjects were asked to place their fingers on four numerically labeled keys on a standard number pad. They were then instructed to repeatedly type a 5-digit sequence (e.g., 4-1-3-2-4) as quickly and accurately as possible during twelve 30 s trials separated by 30 s rest periods (Fig. 3*A*). To minimize the involvement of working memory, the sequence was displayed on a monitor during the typing trials. Subjects were trained on separate sequences with their left and right hands before sleep, with a 10 min break between left- and right-hand training sessions. Following sleep, subjects were tested on the same sequences on the left and right hand, respectively, for 12 trials each with an intervening 10-min break. MST performance in one 30 s trial was calculated as the number of correctly typed sequences. However, in the hospital setting, this measure can yield performance outliers due to inattention, task interruption, or misplacement of the fingers on the keys. To identify and exclude outliers across trials, we followed the procedure in Manoach et al. (84). For each subject and each hand, we fit an exponential model to the learning curve during training and included a constant offset to the exponential model during postsleep testing. If performance on any trial fell more than two SD below the model fit, it was excluded as an outlier. To quantify overnight MST performance change for each hand, we calculated the percentage difference between the mean number of correctly typed sequences in the last three trials of the training session and the mean of the first three valid postsleep trials, following previously published procedures (37). Note that in our dataset this never led to the use of trials beyond the first three for the morning testing session for any subject. MST performance change was averaged across hands when electrophysiology from both hemispheres was available to ensure that each subject contributed only one behavioral measure; otherwise, contralateral performance change was used.

Sleep Oscillation Metrics. We detected slow oscillations, spindles, and ripples in all three regions analyzed and used these detections to estimate average rates (the number of detections divided by the total recording duration in minutes) within each region for each subject. We also measured the co-occurrence rates of slow oscillations, spindles, and ripples across regions, as well as rates of slow oscillation and spindle co-occurrence, slow oscillation and ripple co-occurrence, and spindle and ripple co-occurrence within and across regions. Finally, we calculated the triple-coupling between slow oscillations, spindles, and ripples both within region and across regions, and when possible, averaged this rate across hemispheres. For a visual representation of all 40 occurrences and co-occurrences computed, see Fig. 3*C*.

We define co-occurrence as follows. For slow oscillations, co-occurrence denotes events that occur within ±1 s of the downstate trough; for spindles, co-occurrence denotes events that occur within ±0.5 s of the spindle maximum; for ripples, co-occurrence denotes events that occur within ±0.1 s of the ripple maximum. When calculating co-occurrence between a lower frequency oscillation and higher frequency oscillation, the lower frequency oscillation temporal interval was used to determine event co-occurrence.

To assess the influence of sleep oscillations and epileptic spikes on overnight MST performance change, we partitioned event rates into two categories. In the first category, we selected sleep oscillation events without a co-occurring epileptic spike in any region. To do so, we omitted slow oscillations that co-occurred with an epileptic spike in a [−0.5, 1] s interval around the downstate trough, spindles with an epileptic spike that co-occurred during the spindle duration, and ripples that co-occurred with an epileptic spike in a [−0.5, 0.5] s interval around the peak ripple amplitude. In the second category, we analyzed sleep oscillation events with a co-occurring epileptic spike. To do so, we included sleep oscillation events for which an epileptic spike occurred within the intervals defined for the first category. Finally, we calculated epileptic spike rates within each region as the average spike rate of all channels in a region. In total, we obtained 40 features in the first category of sleep oscillation events without epileptic spikes, 40 features in the second category of sleep oscillation events with epileptic spikes, and 3 epileptic spike rate features (one in each region), yielding a total of 83 features. We estimated univariate Pearson correlations between all features and overnight MST performance change. Additionally, we examined correlations between all predictors and the MST performance change after controlling for epileptic spike rates across the OFC, thalamus, and hippocampus. This involved first building the following linear model for each predictor Y_i, and spike rates OFC_{ES}, $THAL_{ES}$, and $HIPP_{ES}$:

$$Y_i = \hat{\beta}_0 + \hat{\beta}_1 OFC_{ES} + \hat{\beta}_2 THAL_{ES} + \hat{\beta}_3 HIPP_{ES} + e_i,$$

where $\hat{\beta}_0$, $\hat{\beta}_1$, $\hat{\beta}_2$, and $\hat{\beta}_3$ are estimated coefficients. We then used the resulting residuals e_i as the new *residualized* predictor representing information that was not explainable from the spike rates alone.

Partial Least Squares Regression. Given the large number of features (k = 83), the relatively small number of samples (n = 14 subjects), and the high level of correlation among the features, we applied the partial least squares (PLS) regression technique (85) to characterize the relationship between oscillatory coupling and MST performance change. PLS, a multivariate statistical analysis technique robust to highly correlated predictors, has been successfully applied to assess relationships between oscillatory coupling and behavior (86, 87).

PLS is analogous to principal components analysis in that components are created to optimally predict a response (dependent variable). Here, the response Y is the overnight performance change and the predictors X are the 83 sleep

oscillation and epileptic spike features. After standardizing the predictor X and response Y variables, we apply the *plsregress* function in MATLAB which implements the SIMPLS (88) algorithm. SIMPLS iteratively retrieves the first left singular vector (i.e., the vector with the largest eigenvalue) from the decomposition of the matrix $X'Y$, removes the subspace associated with that singular vector from $X'Y$, and repeats the process. Subsequently, a small number of singular vectors are used instead of the original predictors to generate a set of parameter estimates to predict the response Y.

To improve performance of the PLS model, we implemented stability selection (89, 90) as a first step. To select candidate predictors, we computed the univariate correlation between each feature and the response and retained a feature as a predictor in the PLS model if the P-value of the univariate correlation (calculated using a t-statistic with MATLAB's corrcoef function) was $P < 0.1$. We chose the threshold of $P < 0.1$ since univariate correlations do not account for the unique variance explained by each feature in a multivariate model. We applied this predictor stability selection procedure for each leave-one-out subset of samples. The leave-one-out procedure calculated the correlation and p-value between each candidate predictor and the response over 13 samples and repeated this process for each leave-one-out subset. This candidate predictor selection procedure resulted in $n = 14$ sets of candidate predictors, one set for each left out sample. To identify the predictors that occurred consistently across these n sets, we applied a binomial test ($n = 14$, assuming a null probability of 0.10 given the threshold P-value selected) to the n sets of candidate predictors. Doing so resulted in selection of 14 of 83 predictors (*Results*) for analysis. To assess the predictive strength of the PLS model with these selected predictors, we performed leave-one-out cross-validation, training the PLS model on the selected predictors from each subset of $n - 1$ subjects. We applied the PLS model with four singular vectors, though other values for this hyperparameter yielded similar predictive ability for the model. We did not assess performance of the PLS model on any training data as the model is intentionally overfit to these data. We bootstrapped the response over the n PLS model predictions, (i.e., we sampled with replacement from all pairs of predictions and response and recalculated the correlation for each bootstrapped dataset) to estimate the SD for the predictive Pearson correlation.

Statistical Analysis. For the cross-correlation histograms, we tested whether event probabilities were significantly up-regulated or down-regulated relative to baseline (value = 1). To account for multiple comparisons across time bins, we adjusted CI to control the false discovery rate across the 4 s interval and report the mean and FDR-adjusted 95% CI for all instances of up- or down-regulation of event probabilities (91), thus controlling false positives at a 5% rate. Oscillation characteristics were tested using paired t tests and were deemed significant after Bonferroni multiple-comparison correction when appropriate. We used permutation tests to assess the uncorrected P-values of univariate correlations given the small sample size, non-Gaussianity of correlations, and ability to permute subject labels. We used partial least squares regression with predictor selection to predict overnight MST performance change and reported the correlation coefficient (R) between predicted and observed performance change with a bootstrapped CI (*Partial Least Squares Regression*). All statistical tests were two-tailed. Analyses were performed using MATLAB (version R2019b, The MathWorks Inc., Natick, MA).

Data, Materials, and Software Availability. Data needed to reproduce primary figures from this paper and code to reproduce analyses are made available at Zenodo (92). De-identified raw data may be made available to qualified researchers upon reasonable request to the corresponding author, subject to institutional review, applicable ethical approvals, and execution of an appropriate data use agreement.

ACKNOWLEDGMENTS. We thank Erin D. Berja, Katherine G. Walsh, Jonathan F. Huang, Elizabeth A. Kinard, and Skyler K. Goodman for their support in data collection. The authors were supported by NIH NINDS R01NS115868 and the Epilepsy Foundation New England Blue Skies Award.

Author affiliations: [a]Department of Advanced Computing Sciences, Maastricht University, Maastricht 6229 EN, The Netherlands; [b]Department of Neurology, Johns Hopkins University, Baltimore, MD 21205; [c]Department of Neurology, Kennedy Krieger Institute, Baltimore, MD 21205; [d]Department of Neurosurgery, Massachusetts General Hospital, Boston, MA 02114; [e]Harvard Medical School, Boston, MA 02215; [f]Department of Neurology, Massachusetts General Hospital, Boston, MA 02114; [g]Department of Mathematics and Statistics, Boston University, Boston, MA 02215; and [h]Center for Systems Neuroscience, Department of Mathematics and Statistics, Boston University, Boston, MA 02215

Author contributions: A.W., M.A.K., and C.J.C. designed research; A.W., D.C., H.K., and W.S. performed research; D.C., H.K., R.M.R., and M.A.K. contributed new reagents/analytic tools; A.W. analyzed data; R.M.R. enabled data collection; and A.W., M.A.K., and C.J.C. wrote the paper.

1. M. Geva-Sagiv *et al.*, Augmenting hippocampal–prefrontal neuronal synchrony during sleep enhances memory consolidation in humans. *Nat. Neurosci.* **26**, 1100–1110 (2023).
2. J. Kim, A. Joshi, L. Frank, K. Ganguly, Cortical–hippocampal coupling during manifold exploration in motor cortex. *Nature* **613**, 103–110 (2023).
3. C.-F.V. Latchoumane, H.-V.V. Ngo, J. Born, H.-S. Shin, Thalamic spindles promote memory formation during sleep through triple phase-locking of cortical, thalamic, and hippocampal rhythms. *Neuron* **95**, 424–435.e6 (2017).
4. A. Fernández-Ruiz *et al.*, Long-duration hippocampal sharp wave ripples improve memory. *Science* **364**, 1082–1086 (2019).
5. Y. Nir *et al.*, Regional slow waves and spindles in human sleep. *Neuron* **70**, 153–169 (2011).
6. M. Massimini, R. Huber, F. Ferrarelli, S. Hill, G. Tononi, The sleep slow oscillation as a traveling wave. *J. Neurosci.* **24**, 6862 (2004).
7. D. Contreras, A. Destexhe, T. J. Sejnowski, M. Steriade, Spatiotemporal patterns of spindle oscillations in cortex and thalamus. *J. Neurosci.* **17**, 1179–1196 (1997).
8. R. A. Mak-McCully *et al.*, Coordination of cortical and thalamic activity during non-REM sleep in humans. *Nat. Commun.* **8**, 15499 (2017).
9. A. Wodeyar *et al.*, Thalamic epileptic spikes disrupt sleep spindles in patients with epileptic encephalopathy. *Brain* **147**, 2803–2816 (2024).
10. K. Diba, G. Buzsáki, Forward and reverse hippocampal place-cell sequences during ripples. *Nat. Neurosci.* **10**, 1241–1242 (2007).
11. A. G. Siapas, M. A. Wilson, Coordinated interactions between hippocampal ripples and cortical spindles during slow-wave sleep. *Neuron* **21**, 1123–1128 (1998).
12. C. W. Dickey *et al.*, Thalamic spindles and Up states coordinate cortical and hippocampal co-ripples in humans. *PLoS Biol.* **22**, e3002855 (2024).
13. D. Khodagholy, J. N. Gelinas, G. Buzsáki, Learning-enhanced coupling between ripple oscillations in association cortices and hippocampus. *Science* **358**, 369–372 (2017).
14. A. P. Vaz, J. H. Wittig, S. K. Inati, K. A. Zaghloul, Replay of cortical spiking sequences during human memory retrieval. *Science* **367**, 1131–1134 (2020).
15. J. Born, I. Wilhelm, System consolidation of memory during sleep. *Psychol. Res.* **76**, 192–203 (2012).
16. B. P. Staresina, Coupled sleep rhythms for memory consolidation. *Trends Cogn. Sci.* **28**, 339–351 (2024).
17. R. F. Helfrich *et al.*, Bidirectional prefrontal-hippocampal dynamics organize information transfer during sleep in humans. *Nat. Commun.* **10**, 3572 (2019).
18. X. Jiang, J. Gonzalez-Martinez, E. Halgren, Coordination of human hippocampal sharpwave ripples during NREM sleep with cortical theta bursts, spindles, downstates, and upstates. *J. Neurosci.* **39**, 8744–8761 (2019).
19. H.-V. Ngo, J. Fell, B. Staresina, Sleep spindles mediate hippocampal–neocortical coupling during long-duration ripples. *eLife* **9**, e57011 (2020).
20. B. P. Staresina *et al.*, Hierarchical nesting of slow oscillations, spindles and ripples in the human hippocampus during sleep. *Nat. Neurosci.* **18**, 1679–1686 (2015).
21. B. P. Staresina, J. Niediek, V. Borger, R. Surges, F. Mormann, How coupled slow oscillations, spindles and ripples coordinate neuronal processing and communication during human sleep. *Nat. Neurosci.* **26**, 1429–1437 (2023).
22. I. Bozic *et al.*, Coupling between the prelimbic cortex, nucleus reuniens, and hippocampus during NREM sleep remains stable under cognitive and homeostatic demands. *Eur. J. Neurosci.* **57**, 106–128 (2023).
23. N. Maingret, G. Girardeau, R. Todorova, M. Goutierre, M. Zugaro, Hippocampo-cortical coupling mediates memory consolidation during sleep. *Nat. Neurosci.* **19**, 959–964 (2016).
24. C. N. Oyanedel, E. Durán, N. Niethard, M. Inostroza, J. Born, Temporal associations between sleep slow oscillations, spindles and ripples. *Eur. J. Neurosci.* **52**, 4762–4778 (2020).
25. G. Girardeau, K. Benchenane, S. I. Wiener, G. Buzsáki, M. B. Zugaro, Selective suppression of hippocampal ripples impairs spatial memory. *Nat. Neurosci.* **12**, 1222–1223 (2009).
26. M. P. Beenhakker, J. R. Huguenard, Neurons that fire together also conspire together: Is normal sleep circuitry hijacked to generate epilepsy? *Neuron* **62**, 612–632 (2009).
27. M. A. Kramer, S. S. Cash, Epilepsy as a disorder of cortical network organization. *Neuroscientist* **18**, 360–372 (2012).
28. N. Specchio *et al.*, International league against epilepsy classification and definition of epilepsy syndromes with onset in childhood: Position paper by the ILAE task force on nosology and definitions. *Epilepsia* **63**, 1398–1442 (2022).
29. J. K. Kleen *et al.*, Hippocampal interictal epileptiform activity disrupts cognition in humans. *Neurology* **81**, 18–24 (2013).
30. A. B. Silva *et al.*, Interictal epileptiform discharges contribute to word-finding difficulty in epilepsy through multiple cognitive mechanisms. *Epilepsia* **64**, 3266–3278 (2023).
31. S. Henin *et al.*, Spatiotemporal dynamics between interictal epileptiform discharges and ripples during associative memory processing. *Brain* **144**, 1590–1602 (2021).
32. G. L. Holmes, Interictal spikes as an EEG biomarker of cognitive impairment. *J. Clin. Neurophysiol.* **39**, 101 (2022).
33. J. Taylor *et al.*, Patients with epilepsy: Cognitively compromised before the start of antiepileptic drug treatment? *Epilepsia* **51**, 48–56 (2010).
34. M. A. Kramer *et al.*, Focal sleep spindle deficits reveal focal thalamocortical dysfunction and predict cognitive deficits in sleep activated developmental epilepsy. *J. Neurosci.* **41**, 1816–1829 (2021).
35. H. Kwon *et al.*, Association of sleep spindle rate with memory consolidation in children with rolandic epilepsy. *Neurology* **104**, e210232 (2025).

36. B. Frauscher *et al.*, Facilitation of epileptic activity during sleep is mediated by high amplitude slow waves. *Brain J. Neurol.* **138**, 1629–1641 (2015).
37. M. P. Walker, T. Brakefield, A. Morgan, J. A. Hobson, R. Stickgold, Practice with sleep makes perfect: Sleep-dependent motor skill learning. *Neuron* **35**, 205–211 (2002).
38. G. Albouy, B. R. King, P. Maquet, J. Doyon, Hippocampus and striatum: Dynamics and interaction during acquisition and sleep-related motor sequence memory consolidation. *Hippocampus* **23**, 985–1004 (2013).
39. D. Mylonas *et al.*, The effects of eszopiclone on sleep spindles and memory consolidation in schizophrenia: A randomized clinical trial. *Neuropsychopharmacology* **45**, 2189–2197 (2020).
40. M. Sjøgård *et al.*, Hippocampal ripples predict motor learning during brief rest breaks in humans. *Nat. Commun.* **16**, 6089 (2025).
41. P.-C. Chen, J. Stritzelberger, K. Walther, H. Hamer, B. P. Staresina, Hippocampal ripples during offline periods predict human motor sequence learning. *J. Neurosci.* **45**, e1502252025 (2025).
42. B. S. Baxter *et al.*, The effects of closed-loop auditory stimulation on sleep oscillatory dynamics in relation to motor procedural memory consolidation. *Sleep* **46**, zsad206 (2023).
43. P. L. Nunez, R. Srinivasan, *Electric Fields of the Brain: The Neurophysics of EEG* (Oxford University Press, 2006).
44. G. Buzsáki, Hippocampal sharp wave-ripple: A cognitive biomarker for episodic memory and planning. *Hippocampus* **25**, 1073–1188 (2015).
45. C. W. Dickey *et al.*, Cortical ripples during NREM sleep and waking in humans. *J. Neurosci.* **42**, 7931–7946 (2022).
46. A. P. Vaz, S. K. Inati, N. Brunel, K. A. Zaghloul, Coupled ripple oscillations between the medial temporal lobe and neocortex retrieve human memory. *Science* **363**, 975–978 (2019).
47. L. Sheybani, B. Frauscher, C. Bernard, M. C. Walker, Mechanistic insights into the interaction between epilepsy and sleep. *Nat. Rev. Neurol.* **21**, 177–192 (2025).
48. S. Brodt, M. Inostroza, N. Niethard, J. Born, Sleep–A brain-state serving systems memory consolidation. *Neuron* **111**, 1050–1075 (2023).
49. J. G. Klinzing, N. Niethard, J. Born, Mechanisms of systems memory consolidation during sleep. *Nat. Neurosci.* **22**, 1598–1610 (2019).
50. R. A. Swanson *et al.*, Topography of putative bi-directional interaction between hippocampal sharp-wave ripples and neocortical slow oscillations. *Neuron* **113**, 754–768.e9 (2025).
51. J. N. Gelinas, D. Khodagholy, T. Thesen, O. Devinsky, G. Buzsáki, Interictal epileptiform discharges induce hippocampal–cortical coupling in temporal lobe epilepsy. *Nat. Med.* **22**, 641–648 (2016).
52. B. Frauscher *et al.*, Interictal hippocampal spiking influences the occurrence of hippocampal sleep spindles. *Sleep* **38**, 1927–1933 (2015).
53. K. Schiller *et al.*, Focal epilepsy disrupts spindle structure and function. *Sci. Rep.* **12**, 11137 (2022).
54. H. Yu *et al.*, Interaction of interictal epileptiform activity with sleep spindles is associated with cognitive deficits and adverse surgical outcome in pediatric focal epilepsy. *Epilepsia* **65**, 190–203 (2024).
55. A. Sákovics *et al.*, Prolongation of cortical sleep spindles during hippocampal interictal epileptiform discharges in epilepsy patients. *Epilepsia* **63**, 2256–2268 (2022).
56. J. Engel Jr., Concepts of epilepsy. *Epilepsia* **36**, 23–29 (1995).
57. J. D. Shin, S. P. Jadhav, Prefrontal cortical ripples mediate top-down suppression of hippocampal reactivation during sleep memory consolidation. *Curr. Bio.* **34**, 2801–2811 (2024).
58. M. Soula *et al.*, Interictal epileptiform discharges affect memory in an Alzheimer's disease mouse model. *Proc. Natl. Acad. Sci. U.S.A.* **120**, e2302676120 (2023).
59. P.-P. Lenck-Santini, G. L. Holmes, Altered phase precession and compression of temporal sequences by place cells in epileptic rats. *J. Neurosci.* **28**, 5053–5062 (2008).
60. J. N. Gelinas, D. Khodagholy, Interictal network dysfunction and cognitive impairment in epilepsy. *Nat. Rev. Neurosci.* 26, 399–414 (2025).
61. R. J. Porter, J. Kiffin Penry, F. E. Dreifuss, Responsiveness at the onset of spike-wave bursts. *Electroencephalogr. Clin. Neurophysiol.* **34**, 239–245 (1973).
62. S. Vahdat, S. Fogel, H. Benali, J. Doyon, Network-wide reorganization of procedural memory during NREM sleep revealed by fMRI. *eLife* **6**, e24987 (2017).
63. M. P. Walker, R. Stickgold, D. Alsop, N. Gaab, G. Schlaug, Sleep-dependent motor memory plasticity in the human brain. *Neuroscience* **133**, 911–917 (2005).
64. T. C. Rickard, D. J. Cai, C. A. Rieth, J. Jones, M. C. Ard, Sleep does not enhance motor sequence learning. *J. Exp. Psychol. Learn. Mem. Cogn.* **34**, 834–842 (2008).
65. J. Doyon, E. Gabitov, S. Vahdat, O. Lungu, A. Boutin, Current issues related to motor sequence learning in humans. *Curr. Opin. Behav. Sci.* **20**, 89–97 (2018).
66. J. D. Creery *et al.*, Electrophysiological markers of memory consolidation in the human brain when memories are reactivated during sleep. *Proc. Natl. Acad. Sci. U.S.A.* **119**, e2123430119 (2022).
67. L. Kunz *et al.*, Ripple-locked coactivity of stimulus-specific neurons and human associative memory. *Nat. Neurosci.* **27**, 587–599 (2024).
68. Y. Norman, O. Raccah, S. Liu, J. Parvizi, R. Malach, Hippocampal ripples and their coordinated dialogue with the default mode network during recent and remote recollection. *Neuron* **109**, 2767–2780.e5 (2021).
69. G. Umbach *et al.*, Time cells in the human hippocampus and entorhinal cortex support episodic memory. *Proc. Natl. Acad. Sci. U.S.A.* **117**, 28463–28474 (2020).
70. A. S. Lazar, Z. I. Lazar, D.-J. Dijk, Circadian regulation of slow waves in human sleep: Topographical aspects. *NeuroImage* **116**, 123–134 (2015).
71. F. J. van Schalkwijk, R. F. Helfrich, Aperiodic 1/f noise drives ripple activity in humans. *Nat. Commun.* **17**, 746 (2026).
72. M. Mölle, J. Born, "Chapter 7: Slow oscillations orchestrating fast oscillations and memory consolidation" in *Progress in Brain Research* E. J. W. Van Someren, Y. D. Van Der Werf, P. R. Roelfsema, H. D. Mansvelder, F. H. Lopes Da Silva, Eds. (Elsevier, 2011), vol. 193, pp. 93–110.
73. H. Eichenbaum, Prefrontal–hippocampal interactions in episodic memory. *Nat. Rev. Neurosci.* **18**, 547–558 (2017).
74. J. P. Aggleton *et al.*, Hippocampal–anterior thalamic pathways for memory: Uncovering a network of direct and indirect actions. *Eur. J. Neurosci.* **31**, 2292–2307 (2010).
75. U. Eckert *et al.*, Preferential networks of the mediodorsal nucleus and centromedian-parafascicular complex of the thalamus-A DTI tractography study. *Hum. Brain Mapp.* **33**, 2627–2637 (2012).
76. R. P. Vertes, S. B. Linley, W. B. Hoover, Limbic circuitry of the midline thalamus. *Neurosci. Biobehav. Rev.* **54**, 89–107 (2015).
77. A. R. Preston, H. Eichenbaum, Interplay of hippocampus and prefrontal cortex in memory. *Curr. Biol.* **23**, R764–R773 (2013).
78. N. von Ellenrieder, L. Peter-Derex, J. Gotman, B. Frauscher, SleepSEEG: Automatic sleep scoring using intracranial EEG recordings only. *J. Neural Eng.* **19**, 026057 (2022).
79. P. Dahal *et al.*, Interictal epileptiform discharges shape large-scale intercortical communication. *Brain* **142**, 3502–3513 (2019).
80. U. T. Eden, M. A. Kramer, Drawing inferences from Fano factor calculations. *J. Neurosci. Methods* **190**, 149–152 (2010).
81. H. Kwon *et al.*, Sleep spindles in the healthy brain from birth through 18 years. *Sleep* **46**, zsad017 (2023).
82. R. J. Staba, C. L. Wilson, A. Bragin, I. Fried, J. Engel, Quantitative analysis of high-frequency oscillations (80–500 Hz) recorded in human epileptic hippocampus and entorhinal cortex. *J. Neurophysiol.* **88**, 1743–1752 (2002).
83. A. A. Liu *et al.*, A consensus statement on detection of hippocampal sharp wave ripples and differentiation from other fast oscillations. *Nat. Commun.* **13**, 6000 (2022).
84. D. S. Manoach *et al.*, A failure of sleep-dependent procedural learning in chronic, medicated schizophrenia. *Biol. Psychiatry* **56**, 951–956 (2004).
85. A. R. McIntosh, N. J. Lobaugh, Partial least squares analysis of neuroimaging data: Applications and advances. *NeuroImage* **23**, S250–S263 (2004).
86. J. Wu *et al.*, Connectivity measures are robust biomarkers of cortical function and plasticity after stroke. *Brain* **138**, 2359–2369 (2015).
87. J. Wu *et al.*, Utility of EEG measures of brain function in patients with acute stroke. *J. Neurophysiol.* **115**, 2399–2405 (2016).
88. S. de Jong, SIMPLS: An alternative approach to partial least squares regression. *Chemom. Intell. Lab. Syst.* **18**, 251–263 (1993).
89. T. Mehmood, S. Sæbø, K. H. Liland, Comparison of variable selection methods in partial least squares regression. *J. Chemom.* **34**, e3226 (2020).
90. N. Meinshausen, P. Bühlmann, Stability selection. *J. R. Stat. Soc. B Stat. Methodol.* **72**, 417–473 (2010).
91. Y. Benjamini, D. Yekutieli, False discovery rate–adjusted multiple confidence intervals for selected parameters. *J. Am. Stat. Assoc.* **100**, 71–81 (2005).
92. A. Wodeyar *et al.*, Data and code for "A hierarchical cascade of sleep rhythms supports motor memory and is hijacked by epileptic spikes in human epilepsy." Zenodo. https://doi.org/10.5281/zenodo.20592601. Deposited 8 June 2026.